Journal of Catalysis 272 (2010) 158–168

Contents lists available at ScienceDirect

Journal of Catalysis

journal homepage: www.elsevier.com/locate/jcat

Carbon nanofibre-supported palladium catalysts as model hydrodechlorination catalysts

Salvador Ordóñez *, Eva Díaz, Rubén F. Bueres, Esther Asedegbega-Nieto, Herminio Sastre

Department of Chemical and Environmental Engineering, University of Oviedo, Julián Clavería s/n, 33006 Oviedo, Spain

ARTICLE INFO

Article history:
Received 2 December 2009
Revised 19 January 2010
Accepted 1 March 2010
Available online 28 March 2010

Keywords:
Tetrachloroethene
Hydrogenolysis
Carbon activation
Hydrogenation
CNF surface chemistry
XPS speciation

ABSTRACT

Different carbon nanofibre-supported palladium catalysts (Pd/CNF) were prepared and tested for tetrachloroethylene hydrodechlorination. Catalyst properties were varied by changing metal loading (0.5% and 1% wt.), preparation procedure (aqueous or organic solutions), and support chemistry (parent or HNO_3-oxidised CNFs). Fresh and used (during 108,000 s at 0.5 MPa, 523 K, 24 g s $mmol^{-1}$ space time) catalysts were characterised by TEM, XRD, TPD, TPO–MS, nitrogen physisorption, and XPS. Results obtained indicate that the preparation method (using aqueous or organic precursor) plays a key role both in the intrinsic activity of the catalysts (higher for aqueous solutions), and catalyst deactivation (also faster for aqueous solutions).The surface chemistry of the support, influenced by the surface activation and the preparation procedure, markedly affects the Pd^{2+}/Pd^0 ratio (found to be optimal at about 0.3–0.6) and chlorine concentration, these parameters determining the catalysts performance. In general terms, aqueous precursors lead to the highest initial activity (maximum initial TOF of 18 s^{-1}, whereas the maximum initial TOF for catalysts prepared from organic precursor is of 5.6 s^{-1}) and faster deactivation (minimum $TOF_{108,000s}/TOF_0$ of 0.06 and 0.38, respectively). Deactivation causes were observed to be different in both cases: coke formation for the aqueous precursor and chlorine poisoning for the organic-phase precursor.

1. Introduction

Remediation processes based on catalytic hydrodechlorination are considered as emerging technologies for the treatment of organic wastes containing chlorinated compounds [1,2].

Although different catalysts have been tested for this reaction, supported metal catalysts are considered as the most active [3], even in the presence of high amounts of HCl (for example when un-reacted hydrogen is recycled) or when other organic compounds (such as heavier hydrocarbons, organoxygenates or small amounts of organosulphur compounds) are co-processed [4,5]. It is widely accepted that the support plays a key role, especially in the catalyst deactivation. At this point, we have studied the stability of both activated carbon [6] and alumina-supported palladium catalysts [4,7], determining that the formation of carbonaceous deposits, which cause the micropore blockage (especially for the activated carbons), is the main deactivation cause.

Other carbonaceous supports, such as carbon nanofibers (CNF) are receiving increasing attention as support for these catalysts [8]. These materials have a structure based on ordered parallel graphene layers arranged in a specific conformation and are supposed to be less prone to coke formation than inorganic supports, and, at the same time, this coke cannot lead to pore blockage, as in the case of activated carbons. Although it was observed in previous works that these CNFs-based catalysts presented poorer performance than other supported palladium catalysts (mainly because of the poorer catalyst dispersion obtained) [9], their performance is not affected by the support morphology, (as is the case of activated carbons). So, these catalysts are attractive for a better understanding of both the catalytic activity and the deactivation behaviour of hydrodechlorination catalysts.

Likewise, the combined chemical properties of the active phase and the support could give a variety of catalytic functionalities. Since the active species interact in some extent with the support, the catalytic performance of a catalyst strongly depends on a complex mix-up of contributions of the morphology, dispersion of active phase, and electronic properties of the metal [10]. At this point, since the parent CNFs are completely free of surface functional groups, nitric acid treatment over CNF would favour the formation of carboxylic and anhydride groups [11]. The interaction of these surface groups with the Pd particles plays a key role in the Pd catalytic properties. Therefore, in the specific field of hydrodechlorination reaction over carbon-supported Pd catalysts, Amorim et al. [8] demonstrate, studying activated carbons, graphites, and CNFs, that the interaction of the Pd with the support lead to different

* Corresponding author. Fax: +34 985 103 434.
E-mail address: sordonez@uniovi.es (S. Ordóñez).

0021-9517/$ - see front matter © 2010 Elsevier Inc. All rights reserved.
doi:10.1016/j.jcat.2010.03.001

crystallite morphologies and different catalytic activities. Concerning to the catalyst preparation methods, incipient wetness impregnation is the most used on carbon materials. In this way, the medium in which the palladium complexes are introduced into the supports could vary the metal-support interaction. However, there is no consensus on the causes. In this way, Gurrath et al. [12] observed that the nature of the palladium precursor compound and the pre-treatment of the carbon support had a small effect on the resulting dispersion. However, Brunelle [13] observed that the final dispersion of the metal is determined by the repulsion and attraction between charged supports and metal precursors.

The catalytic systems studied were intended to provide valuable information about the structure sensitivity of the reaction in terms of catalyst preparation variables such as the presence of oxygen surface groups over the carbon nanofibre, the metal loading and the method of impregnation of the support. Special attention was also given to deactivation phenomena, which were studied in terms of active phase sintering, formation of coke, and chlorine poisoning of the active phase.

2. Experimental

2.1. Catalysts preparation

A PR-24-HHT carbon nanofibre (free of metallic impurities; <0.2% Fe; 1.95 g/cm^3) was used as a starting material in the reported investigations. The CNF was kindly supplied by Applied Sciences (OH, USA). The parent CNFs were 70 μm length (30–100 μm interval) and 100 nm average diameter (60- to 150-μm interval). A more detailed morphological characterisation of the parent nanofibre, using SEM is provided elsewhere [14].

Parent carbon nanofibres were activated according to the method described in the literature [11]. Succinctly, the starting material was refluxed in 50% nitric acid at 373 K for 48 h and subsequently washed with doubly distilled water in a Soxhlet apparatus. This oxidised CNF is to be referred as "CNF-oxi" throughout the article.

Catalysts were prepared over both supports by wet impregnation method using $PdCl_2$ as precursor, with a palladium nominal load of 0.5% and 1% (wt.). Tested catalysts were prepared by two methods: $PdCl_2$ solved in either an aqueous solution of HCl 0.1 N (aqueous method, "aq") or isopropanol (organic method, "org"). For the aqueous method, the impregnation solution consisted on $PdCl_2$ dissolved in 0.1 N HCl to generate H_2PdCl_4, with a solution volume exceeding by 20% the pore volume of the support in each case. This precursor solution was dissolved in 60 cm^3 of 0.1 N HCl. One gram of the carbon nanofibre was added to this solution in a flask under stirring with a magnetic stirrer for 600 s. The flask was then placed in a rotavapor equipped with a water bath at 343 K, spun, and vacuum pumped for 1800 s. Next, the powder was dried in an oven at 383 K for 7.2×10^3 s. In the case of organic method, the desired amount of $PdCl_2$ was dissolved in 60 cm^3 of isopropanol, being the impregnation and drying steps performed as in the other case. Finally, catalysts were pelletised, crushed, and sieved (selecting particles in the interval 60–100 μm) in order to avoid diffusional artefacts and high pressure drops in the catalytic bed.

2.2. Reaction studies

Reactions were carried out in a fixed-bed reactor consisting of a 9 mm internal diameter, 500-mm-length stainless steel cylinder. More details about the catalytic reactor and operating conditions are given elsewhere [6,7,15]. The catalyst (in most experiments 0.25 g) mixed with glass was placed in the mid-section of the reactor (5–10 mm) over a double metallic grid introduced inside the reactor (mesh size 60 μm). The bottom and top sections of the reactor were packed with glass spheres, the upper section being used as pre-heating zone. The catalyst was activated *in situ* before use by passing through the reactor 0.01 L s^{-1} (s.t.p.) of hydrogen at 523 K and 0.5 MPa for 9×10^3 s. In the case of the catalysts prepared using the parent CNF as support, with 0.5% Pd loading, and prepared using organic precursor, another two reduction temperatures (400 and 673 K) were tested in order get a wider interval of active phase dispersions. The same reduction procedures were used to obtain catalyst samples for further characterisation.

Catalytic experiments were carried out at 0.6 MPa and 523 K. The organic feed (toluene as solvent and tetrachloroethylene, supplied by Panreac with a minimum purity of 99.5% and 99.9%, respectively) flowed downwards through the reactor, pumped by an Alltech 525 liquid chromatography pump. A flow rate of 12 L s^{-1} was fixed, with molar feed flow rate of TTCE of 0.0105 mmol s^{-1}, corresponding to a space time of 24 g s mmol^{-1} of reactant. At reaction conditions, the organic feed was completely vaporised. Hydrogen (with a H_2/TTCE ratio of 90, in order to ensure that hydrogen is not a limiting reactant) was fed co-currently, the flow rate being controlled by a Brooks 5850 TR/X mass-flow regulator.

Reaction products were automatically analysed (reported value is the average value of three consecutive injections when analytic reproducibility better than ±5%) by capillary GC in a Shimadzu GC-2010 apparatus equipped with a FID detector, using a 15-m-long WCOT silica-fused capillary column as stationary phase. Peak assignment was performed by GC–mass spectra, and responses were determined using standard calibration mixtures. Once the reaction was stopped, catalysts were cooled to room temperature under nitrogen flow and stored in inert atmosphere.

Hydrogen chloride concentration was measured by absorption of the gas in distilled water and titration of the resulting solution with NaOH. Chlorine mass balance (considering the chlorine content of the TTCE feed and the chlorine in the TTCE and HCl at the reactor outlet) presents closures higher than 95% in all the experiments reported in this work.

The presence of both internal and external mass transfer limitations, as well as intraparticle and bed thermal profiles, in the experiments reported in this work is discarded. These effects were experimentally (working with different particles sizes, catalyst/inert ratios, and gas velocities but keeping constant the space time) and theoretically ruled out in previous studies carried out with this reactive system, working at the same concentrations and operation conditions but with commercial Pd/Al_2O_3 and Pd/activated carbon catalysts of higher dispersion, internal porosity, and intrinsic activity (and hence more prone to be limited by mass-transfer effects) [7].

In order to determine the influence of spill-over effects caused by CNF functional groups, additional experiments were carried out with the 1% Pd/CNF prepared by the organic method, but diluting the catalyst with either the parent CNF or the oxidised CNF (25% of catalyst, 75% of nanofiber). Both materials were intimately mixed, grinded, pelletised, crushed, and sieved. Experiments were done using one gram of these mixtures, so that the space velocity, expressed as mol of TTCE fed per second and exposed palladium atom, was the same than in the previously described experiments.

2.3. Catalysts characterisation

The textural characterisation of the materials, specific surface area and pore volume, was based on N_2 adsorption isotherms, determined with a Micromeritics ASAP 2000 surface analyser. The morphology of the catalysts was studied by scanning electron microscopy (SEM) using a Jeol JSM-6100 microscope; the sample

was deposited on a standard aluminium SEM holder and gold coated. Powder X-ray diffraction (XRD) was performed with a Philips PW1710 diffractometer, working with the Cu Kα line (λ = 0.154 nm). Measurements of the samples were carried out in the range 2θ of 35–45°, at a scanning rate of 0.002° in 2θ min^{-1} in order to study the active metal, as the (1 1 1) crystallographic plane of Pd diffract the X-ray beam at 40.1°. For applying the Scherrer equation, the instrumental broadening of the peaks has been corrected using α-silicon (99.9999%) as standard. Likewise, the Pd particle morphology and size distributions were determined by transmission electron microscopy (TEM) in a JEOL JEM2000EXII microscope and by CO chemisorption in a volumetric Micromeritics ASAP 2020 apparatus. Methodology used for estimating crystallite size (measuring 200 individual crystallites) is described in detail in a previous work [5], whereas a 1:1 stoichiometry was tentatively considered for CO chemisorption.

Carbon support structural characteristics as well as the carbonaceous deposits after reaction were characterised by temperature-programmed reduction (TPD) and oxidation (TPO), employing a Micromeritics TPD-2900 apparatus connected to a Pfeiffer Vacuum-300 mass spectrometer. For this purpose, 10 mg carbon sample was maintained in a helium stream (TPD) or an oxygen-stream – 2% O_2/98% He – (TPO) at 323 K for 1800 s, with a flow rate of 0.83 cm^3 s^{-1}, and heated from 323 to 373 K at 0.16 K s^{-1}.

The chemical composition of the fresh (after reduction in H_2 at 523 K for two hours) and used catalysts was studied by X-ray photoelectron spectroscopy (XPS). XPS experiments were carried out on a SPECS-PHOIBOS system equipped with a hemispherical electron analyser operating in a constant pass energy, using Mg Kα radiation ($h\nu$ = 1253.6 eV). The samples were fixed to the sample holder using a carbon adhesive tape and analysed without further treatments. The background pressure in the analysis chamber was kept below 2×10^{-9} mbar during data acquisition. Since samples are conductors (could be confirmed on observing the position of the C1s peak at 284.6 eV), there was no need of applying surface neutralisation during measurements. Assignation of binding energies to different atoms and oxidation states has been done according to literature recommendations [16]. Quantification results reported are the average of the measurement of at least five different zones in the sample.

Hydrogen adsorption/desorption experiments for both supports and the prepared catalysts were performed using a thermogravimetric analyser (TG, Setarsam-Sensys 16 Evolution) with a vacuum system. Experiments were performed according to procedure proposed by Chen and Huang [17], involving vacuum treatment of the sample, reduction at 523 K and recording of a desorption–adsorption cycle by heating the sample in an hydrogen flow from 303 to 473 K (at 5 K/min) and a subsequent cooling down to 303 K. Buoyancy effects and adsorption by corundum sample holder were corrected using a blank calibration. In general terms, adsorption–desorption process was found to be reversible, adsorption data provided corresponding to the final adsorption step.

3. Results

3.1. Characterisation of fresh catalysts

The textural and physicochemical properties of the parent and modified carbon nanofibres are detailed in previous works [11,14]. Nitric acid treatment leads to a slight increase in the surface area, whereas increasing amounts of CO and CO_2 releases during TPD experiments were observed, with an important relative contribution of carboxylic and anhydride groups to the surface chemistry of the oxidised nanofibre. In the previous work, devoted to study the effect of the CNF chemical activation on its adsorption properties [11], it was observed that these functional groups play a key role on the adsorption properties of the CNFs. XPS analysis of catalysts prepared from both supports indicated that no significant modifications in the concentration of oxygen surface groups took place during catalysts preparation procedure. The results obtained in the characterisation of the prepared catalysts are shown in Table 1. Surfaces areas and pore volume do not vary for the catalysts prepared from the parent CNF (around 32 m^2 g^{-1} and 0.16 cm^3 g^{-1}). By contrast, a slight loss of BET surface area and pore volume occurred during impregnation of the oxidised support (whose surface area and pore volume are 38 m^2 g^{-1} and 0.21 cm^3 g^{-1}, respectively), which can be attributed to variations of the morphology of the fibres during the preparation.

The surface chemistry of the materials has been characterised by TPD, according to the procedure outlined in [11]. The CO and CO_2 profiles for the parent CNF, the oxidised CNF and the oxidised CNFs with a 1% Pd are depicted in Fig. 1. It is observed, for the catalyst prepared from oxidised nanofibres, that the CO and CO_2 releases are very similar (in both cases, using organic and aqueous precursors) to the parent-oxidised nanofibres, suggesting that the surface chemistry of the surface remain almost unaltered.

Three different techniques have been used for estimating the palladium dispersion. Carbon monoxide chemisorption offers reproducible results (shown in Table 1), but this technique is not applicable to the 0.5% Pd catalysts because of experimental limitations (CNF density is very low, being not possible to load enough

Table 1
Morphological properties (measured by nitrogen physisorption), average crystallite size (measured by TEM, CO chemisorption, and XRD), hydrogen adsorption capacity (measured by TG in H_2 at 0.1 MPa), and Pd/C Cl/Pd and Pd^{2+}/Pd ratios measured by XPS for the fresh reduced Pd/CNF catalysts tested in this work. Catalysts were reduced at 523 K, unless otherwise mentioned.

Catalyst	S_{BET} (m^2 g^{-1})	Mesopore volume (cm^3 g^{-1})	d_{XRD} (nm)	d_{TEM} (nm)	d_{CO} (nm)	Pd/C (%, w/w)	Cl/Pd (%, w/w)	Pd^{2+}/Pd^0 (%, w/w)	H_2 uptake (%, w/w)
0.5% Pd–CNF-aq	32.3	0.16	30			0.6	1.5	0.23	0.037[c]
1% Pd–CNF-aq	32.6	0.16	30	27	31	1.0	1	0.22	0.045[c]
0.5% Pd–CNF-oxi-aq	35.6	0.21	30			0.55	2.5	0.28	0.083[d]
1% Pd–CNF-oxi-aq	35.3	0.21	30	26	33	0.98	1.2	0.61	0.103[d]
0.5% Pd–CNF-org	32.6	0.16	23			0.55	2	0.28	0.039[c]
1% Pd–CNF-org	33.0	0.18	28	24	28	1.02	2.6	0.66	0.056[c]
0.5% Pd–CNF-oxi-org	36.1	0.21	29			0.58	2.8	0.41	0.023[d]
1% Pd–CNF-oxi-org	35.3	0.21	30	29	30	1.06	3.4	0.33	0.026[d]
0.5% Pd–CNF-org[a]	32.5	0.17	21			0.54	3.5	0.78	n.a.
0.5% Pd–CNF-org[b]	32.2	0.15	26			0.55	1.2	0.16	0.035[c]

[a] Catalyst reduced at 400 K.
[b] Catalyst reduced at 673 K.
[c] Adsorption capacity of the support: 0.055%.
[d] Adsorption capacity of the support: 0.020%.

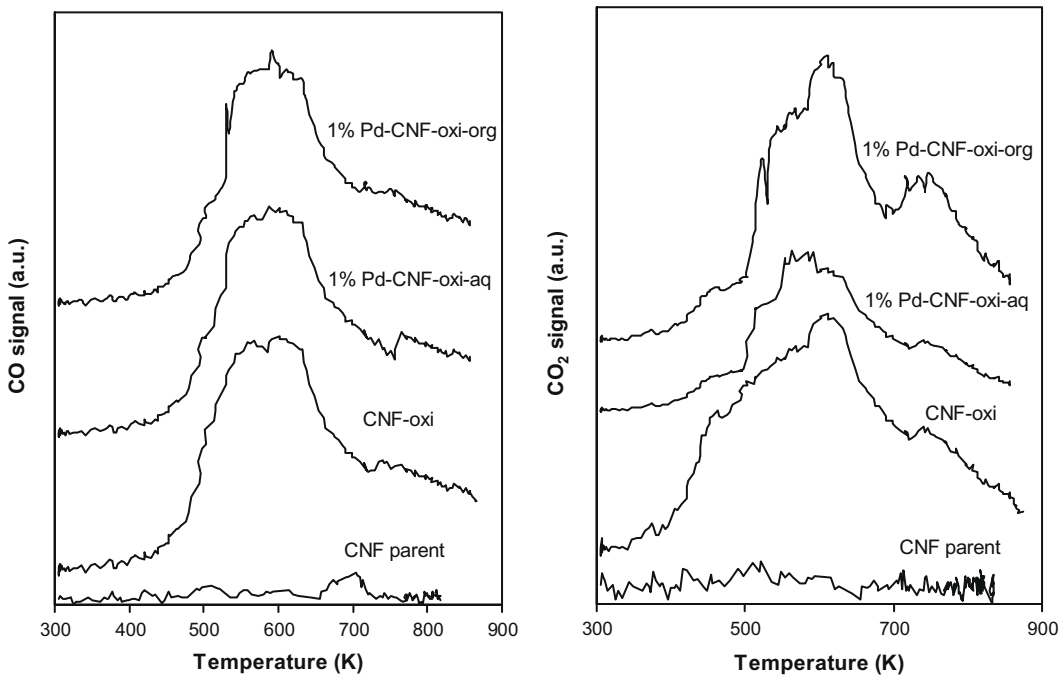

Fig. 1. CO (left) and CO_2 (right) releases during the TPD of the parent CNF, the oxidised CNF (CNF-oxi), and catalysts 1% Pd/CNF-oxi prepared from aqueous and organic precursor.

amount in the sample tube for obtaining accurate measurements). Considering this fact and the low reproducibility of this technique for used catalysts (since both chlorine and carbonaceous deposits hinder CO chemisorption), alternative procedures for measuring metal dispersion were needed. TEM micrographs were also used for estimating metal dispersion. Although the metal particles present a regular hemispherical geometry in all the cases, it is difficult to obtain accurate crystallite size distributions histograms because of the poor particle-support contrast when particles are close to the external border of the nanofibre [18] and the low volumetric concentration of the active phase (specially with 0.5% loadings). The third technique for being considered is the Scherrer analysis of the XRD profiles (1 1 1 diffraction peak of Pd, represented in Fig. 2). This technique is considered as very accurate for crystallite sizes larger than 2 nm [19], and it is also considered as non-sensitive to chemical changes in the crystallite surface (such a formation of carbides or chlorides) [20]. If the results of the three techniques are compared (Table 1), it is observed that they are in a reasonable agreement. Although dispersions reported in the literature present important variations, depending on CNF nature and impregnation method, dispersion values obtained are in a good agreement with that reported in the literature for materials prepared following similar procedures (see for example, [8]).

It is remarkable that the catalysts prepared from aqueous solution present an average crystallite size of 30 nm, independent of the CNF treatment, whereas more significant variations were found for the catalysts prepared from organic solution. Our results are in a good agreement with the results reported by Hermans et al. [21] who reported the highest Pd dispersion over CNF-based catalysts when organic solvents (as isopropanol) are used for preparing the precursor solutions. These authors stated that this effect is caused by the high hydrophobic character of the CNF, even when they are chemically activated. Concerning to the interaction of the palladium precursor ($PdCl_4^{2-}$) with carbon supports, there are not agreement in the literature about which kind of interaction is more important: the electrostatic interaction with ionised functional groups [22–24] or with the electropositive carbon atoms of the functional groups [24]. Our results suggest that this kind of effects is not very important, probably because of the lower concentration of functional groups, especially when compared with activated carbons [25].

Samples of the 0.5% Pd/CNF-org were reduced at other two different temperatures (400 and 673 K) in order to obtain a wider interval of metal dispersions. Thus, the resulting catalysts have an average crystallite size of 21 and 26 nm, respectively, whereas the catalyst reduced at 523 K has an average Pd crystallite size of 23 nm.

From XPS experiments, in addition to the surface Pd concentration, data of Cl/Pd and Pd^{2+}/Pd^0 of the catalysts were obtained (Table 1). Analyses of the catalysts reveal the presence of chlorine from palladium precursor. In all cases, the chlorine appears in a binding energy region corresponding to inorganic chlorine (198–199 eV). Although this chlorine precursor is considered to promote catalyst sintering or poisoning, this contribution seems to be irrelevant in our case, because of the large amounts of HCl released during the reaction [9]. Likewise, it is observed that the Pd^{2+} fraction is higher for the oxidised support based catalysts and for the impregnation with isopropanol. In general terms, higher chlorine concentrations are observed for the catalysts prepared from organic solution and, less markedly, for the catalysts prepared on oxidised support.

If it is considered that the chlorine comes from the HCl generated during the palladium particles reduction, it is inferred that although the chlorine ions trend to be concentrated on the metal surface the functional groups of the support can promote the adsorption of this chlorine [12,26]. Thus, our results suggest that this interaction is favoured when the CNF is oxidised (higher interaction with a polar molecule) and when an organic solution is used. In this last case, although the causes are unclear, they seem to be controlled by the kinetics of the HCl formation, which is related to the used solvent [10]. Concerning to the effect of the reduction temperature, it was observed that as expected the Pd^{2+}/Pd ratio and the Cl/Pd ration decreases as reduction temperature increases.

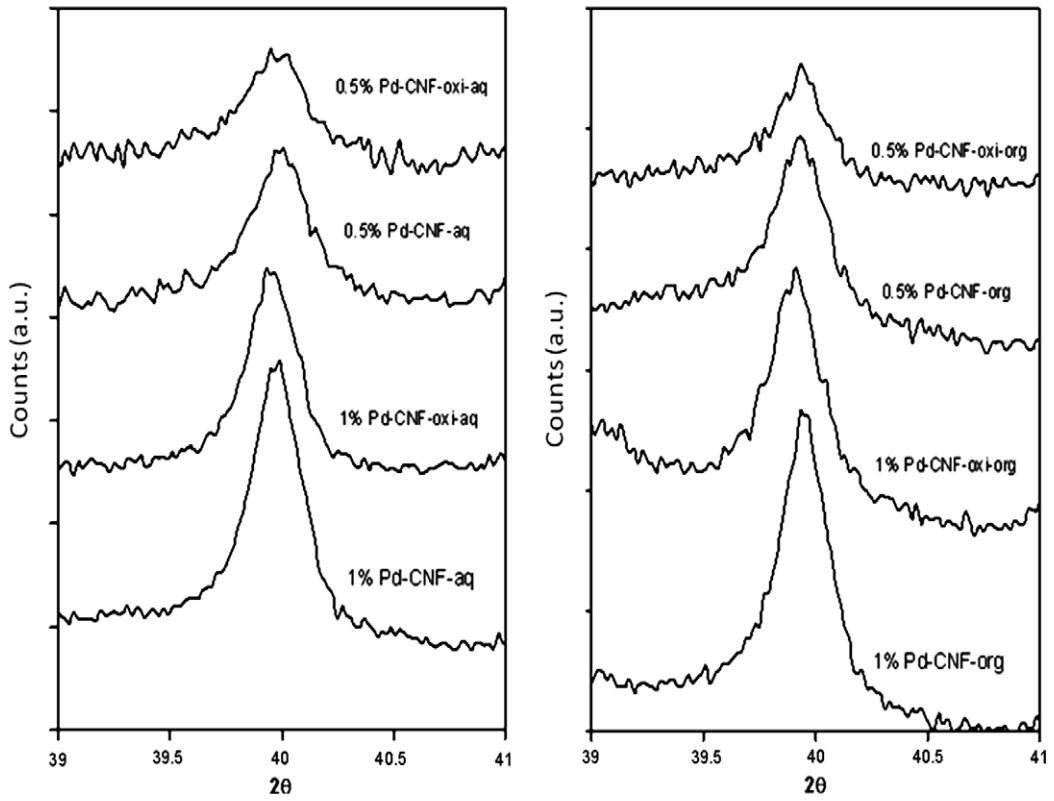

Fig. 2. XRD diffractograms of the fresh reduced catalysts used in this work in the window of the Pd 1 1 1 diffraction peak (peak used for estimating Pd crystallite size).

Thermogravimetric hydrogen adsorption experiments (also summarised in Table 1) reveal that both the presence of functional groups on the support surface and the preparation method largely affect the adsorption properties of the material. Therefore, the adsorption capacity of the nanofibre is reduced upon activation (0.055% vs. 0.020%), suggesting that the presence of these active groups hinders the adsorption of the hydrogen, in good agreement with literature findings [27]. Concerning to the effect of the metallic palladium on adsorption properties, this effect depends on the presence/absence of functional groups. In the case of the parent nanofibres, the presence of palladium leads to slight variations in the hydrogen adsorption capacity. For the activated nanofibres, the effect of the Pd strongly depends on the preparation method. Therefore, adsorption capacity of the catalysts prepared from aqueous precursor is more than five times higher than the corresponding to the oxidised support.

3.2. Catalytic performance

Pd–CNF catalysts were tested in the hydrodechlorination of tetrachloroethylene, catalyst performance is expressed in terms of conversion of TTCE, defined as the percentage of TTCE fed to the reactor which is reacted. Fig. 3 shows the evolution of the conversion with the time for the catalysts with 0.5% and 1% wt. of Pd. All the curves reported in this figure have been replicated in order to ensure the reproducibility of the obtained data. In general terms, good reproducibility has been obtained (conversions in the range ±5%), even using catalysts prepared in different batches. Methylcyclohexane was the only reaction product derived from the solvent, being only observed (and at very low concentrations) during the first reaction minutes.

In general trends, the behaviour of the catalysts largely depends on the preparation method. Catalysts prepared from aqueous precursor present higher initial activity and faster deactivation than the catalysts prepared using organic precursor. Concerning the selectivity, trichloroethylene (TCE) is the only intermediate product detected, since the reactions of decomposition of other intermediates are very fast [7]. In all cases, the selectivity to TCE is very low, below 5%.

In the case of the Pd/CNF reduced at different temperatures, it was observed that the catalyst reduced at the highest temperature show better performance both in terms of initial activity and deactivation behaviour than the catalyst reduced at 523 K. By contrast, the catalyst reduced at the lowest temperature (400 K) is slightly more active than the catalyst reduced at 523 K and presents very similar deactivation pattern.

Experiments carried out with the mechanical mixtures of the 1% Pd/CNF-org and parent or oxidised nanofibres provide very different results. No noticeable effect was observed when the catalyst was diluted with the parent nanofibre, whereas the catalyst performance is clearly enhanced when the catalyst was diluted with the oxidised carbon nanofibre.

3.3. Characterisation of used catalysts

Since all the catalysts tested in this work showed deactivation after 108,000 s on stream, the used catalysts were also characterised in order to elucidate the deactivation causes. SEM micrographs (not shown) reveal that the morphology of the catalysts remains unaltered during the reaction. Surface analysis (XPS) of the catalysts (Table 2) did not reveal any significant Pd losses during the reaction.

The evolution of the crystallite size presents two marked trends. The catalysts prepared over the parent CNF exhibit important sintering effects, being more important for the highest metal loading (Table 2), whereas the catalysts prepared over the oxidised support show this effect at lower extent. These results suggest that the absence of functional groups on the catalyst surface leads to a weaker

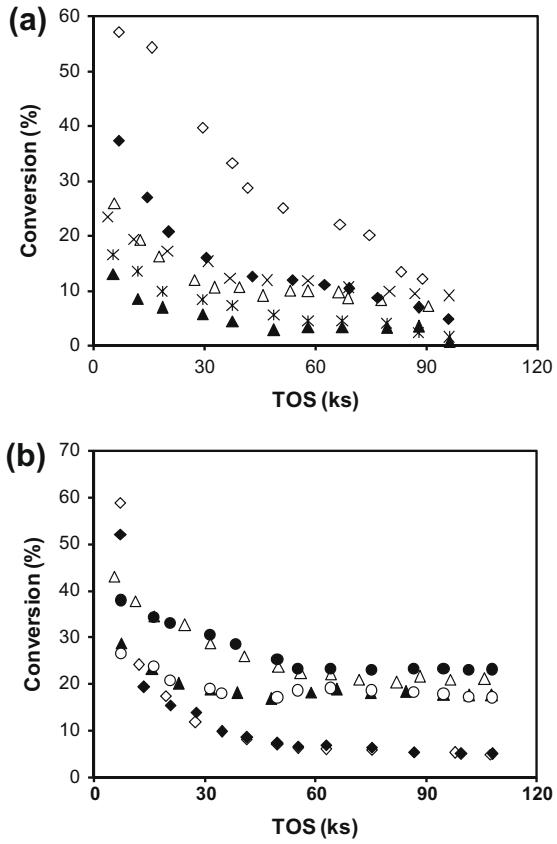

Fig. 3. Evolution of TTCE conversion with time on stream for the hydrodechlorination of TTCE at 250 °C over the catalysts with 0.5% (a) and 1% (b) of Pd loading, using the following supports and preparation methods (see codes in Section 2.1): (♦) CNF-aq; (◇) CNF-oxi-aq; (▲) CNF-org; (△) CNF-oxi-org; (●) CNF-org + CNF-oxi (25% of catalyst); (○) CNF-org + CNF (25% of catalyst); (X) CNF-org reduced at 673 K; (*) CNF-org reduced at 400 K.

Table 2
XRD average crystallite diameter, Pd/C (w/w ratio), Pd^{2+}/Pd ratio, percentage of inorganic (binding energy between 198 and 199 eV) and organic (binding energy between 199.5 and 201 eV) chlorine, and Cl/Pd (total chlorine) ratio for the studied catalysts after 108,000 s on stream at 523 K and 0.5 MPa. Catalysts were reduced at 523 K, unless otherwise mentioned.

Catalyst	d_{XRD} (nm)	Pd/C (w/w)	Pd^{2+}/Pd^0	Cl_{org}/Cl_{total}	Cl_{inorg}/Cl_{total}	Cl/Pd
0.5% Pd–CNF-aq	38	0.66	1.38	0.23	0.77	10.5
1% Pd–CNF-aq	52	0.94	2.27	0.21	0.79	9.6
0.5% Pd–CNF-oxi-aq	35	0.59	3.70	0.24	0.76	21.6
1% Pd–CNF-oxi-aq	35	0.97	2.28	0.14	0.86	5.2
0.5% Pd–CNF-org	40	0.55	4.49	0.07	0.93	9.6
1% Pd–CNF-org	46	0.98	1.54	0.11	0.89	9.9
0.5% Pd–CNF-oxi-org	38	0.54	3.17	0.06	0.94	20.1
1% Pd–CNF-oxi-org	38	1.05	1.46	0.10	0.90	16.5
0.5% Pd–CNF-org[a]	42	0.54	14.1	0.05	0.95	27.7
0.5% Pd–CNF-org[b]	43	0.55	1.62	0.15	0.85	8.46

[a] Catalyst reduced at 400 K.
[b] Catalyst reduced at 673 K.

interaction of the metal particles with the support, thus, the probability of crystallite coalescence increases as the metal concentration increases. The effect of the functional groups of carbonaceous materials on the Pd dispersion has been also observed by other authors. For example, Calvo et al. [27] observed that the presence of CO_2-evolving oxygenated functional groups (groups also present on the oxidised materials studied here [11]) plays a key role in the dispersion of the prepared catalysts. In our case, the interaction between these functional groups and Pd particles seems to avoid the sintering. On the other hand, the hydrogen chloride released during the reaction plays an important role in the coalescence–redispersion of the metal particles, through the formation of volatile chlorides [28]. At first insight, it could be contradictory that the presence of these functional groups affects the evolution of the dispersion during the reaction but not during preparation (similar metal dispersions with both kinds of supports). However, it must be taken into account that the final palladium dispersion in the fresh catalysts largely depends on the chemistry of the chlorine–palladium complexes and the kinetics of the transformation of the precursor in the reduced metal. At this point, volatility properties of Pd–Cl complexes (which do not depend on support properties) can play a key role in the final dispersion of the catalyst [10].

XRD patterns of the fresh and used catalysts do not show significant differences for the organic impregnated catalyst. In the case

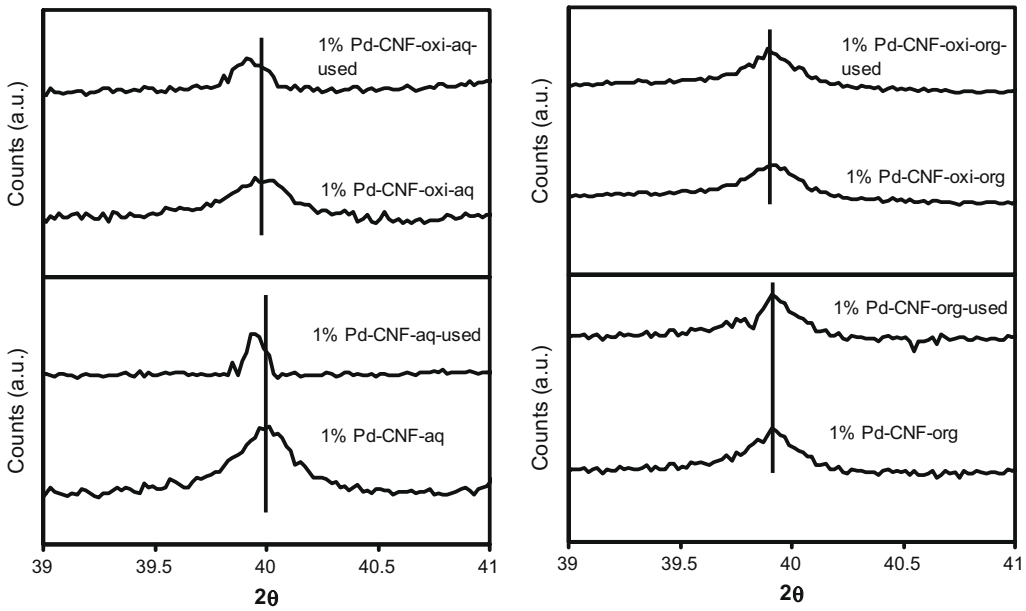

Fig. 4. Comparison of the XRD patterns in the window of the 1 1 1 Pd diffraction peak for the four 1% Pd/CNF before and after 108,000 s on stream. Left plot: prepared from aqueous precursor. Right plot: prepared from organic support.

of the aqueous impregnated catalysts, as observed in the Fig. 4 for the 1% Pd-loaded nanofibres, a slight displacement ($2\theta = 0.04°$) is observed for all the used catalysts. This displacement was attributed by other authors [29,30] to the formation of palladium carbide by the interaction with carbonaceous deposits on the metal surface. In order to study more thoroughly the presence of these coke deposits, TPO analyses of the catalysts were carried out. Two peaks (for the CO_2 evolved) are observed for the used catalysts prepared form aqueous precursor (the TPO profile for the used 1% Pd/CNF-oxi-aq is shown in Fig. 5): the main peak, at around 1033 K, corresponding to the combustion of the carbon nanofibre supports; and another peak at around 750 K, which is related to the burning of carbonaceous deposits [31]. It should be noted that TPO analyses of both the parent and the activated nanofibres were carried out in a previous work [11], being observed in both cases the presence of only one bulk combustion peak (similar to the second peak observed in Fig. 5). The coke deposit combustion peak is exclusively observed in the aqueous impregnated catalysts, not existing evidences of carbonaceous deposits for catalysts prepared using organic solutions. For 1% of nominal Pd loading, the percentage of coke per weight of catalyst, determined from peak area, was 1.70% for the CNF support and 1.20% for the oxidised CNF; whereas for the 0.5% of nominal load, the small area of the coke combustion peak prevents an accurate quantification. Although temperatures reported in the literature for combustion of coke deposits formed over Pd crystallites are lower (533–563 K [6,31,32]), these values correspond to catalysts supported on alumina or activated carbon supports. In these cases, support acid sites or organic functional groups may catalyse the coke deposition; thus, it would be much more distributed and, therefore, it could be more accessible for oxidation. In the case of CNFs, this effect is not taking place because of the high chemical inertness of the support. The amount of coke in the catalysts made from oxidised support is lower than the corresponding to the parent one. This result suggests that these functional groups do not catalyse the formation of coke.

In order to estimate the changes on the catalyst chemistry during the reaction, surface analyses of the used catalysts were performed by XPS (summarised in Table 2). The original Pd 3d core level spectra for two representative catalysts and the fit of the curves are shown in Fig. 6. Main XPS parameters for Pd $3d_{5/2}$ and Cl $2p_{3/2}$ core levels of both the fresh and used catalysts are summarised in Table 2. The original Pd 3d core level spectrum for the fresh catalysts reveals the existence of two Pd species: Pd in its reduced (Pd^0) [33,34] and oxidised (Pd^{2+}) state [17,34,35]. The used catalysts also exhibit peaks due to Pd^0 and Pd^{2+} species, although the Pd^{2+}/Pd^0 ratio is much higher in the catalysts after reaction. Concerning to chlorine, two different species are found on the surface of the used catalysts [36,37]: chloride anions, Cl $2p_{3/2}$, and chlorine covalently bonded to carbon (Table 2).

In order to ensure the presence of functional groups in the oxidised CNF-based catalysts, TPD of the used samples were performed. Comparing the CO and CO_2 releases of these samples (depicted in Fig. 7 for the 1% Pd catalysts) with the corresponding

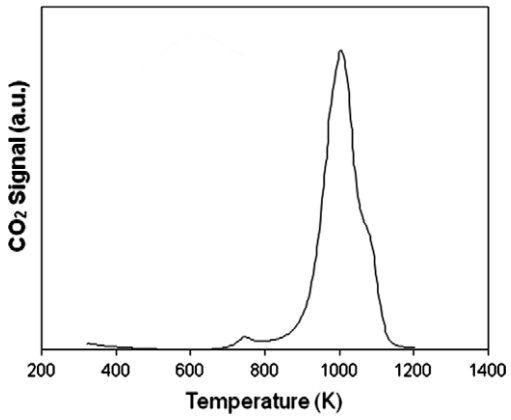

Fig. 5. CO_2 release profile during the TPO of the used 1% Pd/CNF-oxi-aq catalyst. Heating rate: 0.16 K s^{-1}.

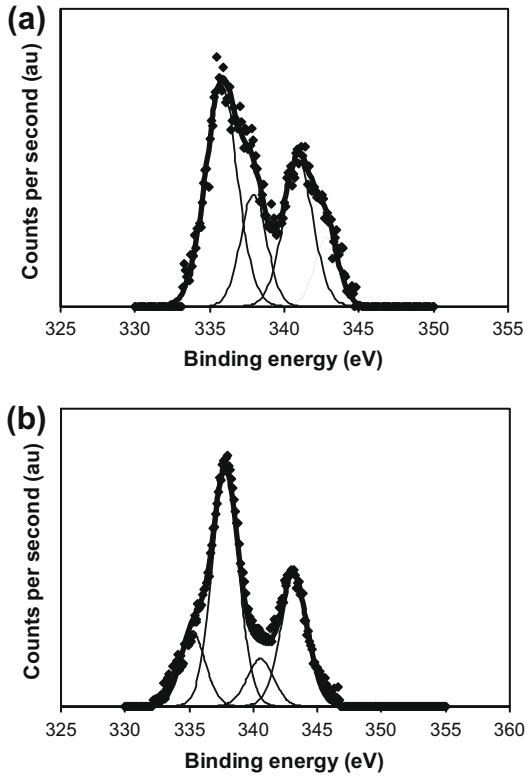

Fig. 6. Pd 3d core level spectra of: (a) fresh 0.5% Pd–CNF-oxi-org and (b) used 0.5% Pd–CNF-oxi-org.

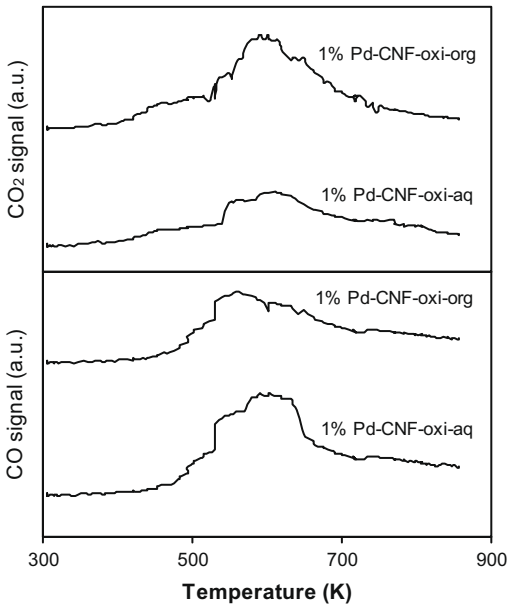

Fig. 7. CO (lower plot) and CO_2 (upper plot) releases during the TPD of 1% Pd/CNF-oxi-org catalysts before and after 108,000 s on stream for TTCE hydrodechlorination.

to the fresh catalysts, it is observed that the functional groups and therein the surface chemistry of the supports remains almost unaltered, concluding that the effect of these functional groups on catalyst performance takes places during all the reaction.

4. Discussion

Results obtained can be discussed both in terms of the initial activity and the steady-state activity (Table 3). The first parameter allows gaining further understanding into the intrinsic activity of the catalysts, whereas the second one provides new insights into the activity of the catalysts at the operation conditions. In order to compare the intrinsic activity of the catalyst, initial TOF values, that is, the number of TTCE molecules reacted per Pd-exposed atom and per time, were calculated for all the studied catalysts, considering the conversion extrapolated to zero hours on stream and the palladium dispersion of the fresh catalysts. Dispersion was calculated from the average crystallite diameter reported in Table 1, using the Pd crystallographic parameters reported in the literature [38]. TOF values are selected for comparison because they allow comparing the catalytic activity in absence of deactivation effects. Although there are not, to the best of our knowledge, TOF values reported for TTCE hydrodechlorination at these reaction conditions, TOF values reported in this work are higher than TOF values reported in the literature for similar reactions. So, Lambert et al. reported TOF of 0.05 s^{-1} for the hydrodechlorination of 1,2,-dichloroethane at 473 K over Pd/SiO_2 catalyst [39], whereas Sánchez et al. reported TOF of 0.03 s^{-1} for dichloromethane hydrodechlorination over Pd/Al_2O_3 catalysts at 473 K [40]. Both compounds are largely less reactive than TTCE for hydrodechlorination reactions [6]. In the case of chloro-olefins, Nutt et al. reported a TOF of 0.004 s^{-1} for liquid-phase trichloroethylene hydrodechlorination at ambient temperature [41]. The observed differences in TOF values are caused by both the highest reactivity of the TTCE and because the TOF values reported in this work are referred to the fresh catalysts, not to the steady-state catalyst.

Initial TOF was correlated to different parameters, such as crystallite size, Pd^{2+}/Pd^0 ratio or Cl/Pd concentration. The evolution of the TOF with the particle diameter (Fig. 8) shows very different behaviour depending on the preparation method. In the case of the catalysts prepared from organic precursors, TOF slightly increases as the particle diameter increases, suggesting that the reaction is structure sensitive. There is no general agreement about the structure sensitivity of the hydrodechlorination reaction on palladium catalysts. Several authors working with different chlorinated compounds and palladium catalysts have found that an increase in dispersion leads to a decrease in the intrinsic activity [42]; however, other authors [43] reported the opposite behaviour. According to the classical theory on structure–sensibility reactions, structure sensitivity is caused by either geometrical, electronic, or coordination chemistry effects, which are not important at crystallite sizes higher than 2 nm [44,45]. However, it is also stated that the presence of other factors, such as surface reconstructions, can lead to similar effects for larger crystallites, as suggested by Dumesic et al. for explaining the structure sensitivity of Fe/MgO (30 nm) when used as catalysts for ammonia synthesis [46]. This kind of behaviour is associated with the formation of volatile species, such as iron nitrides or palladium halides [47].

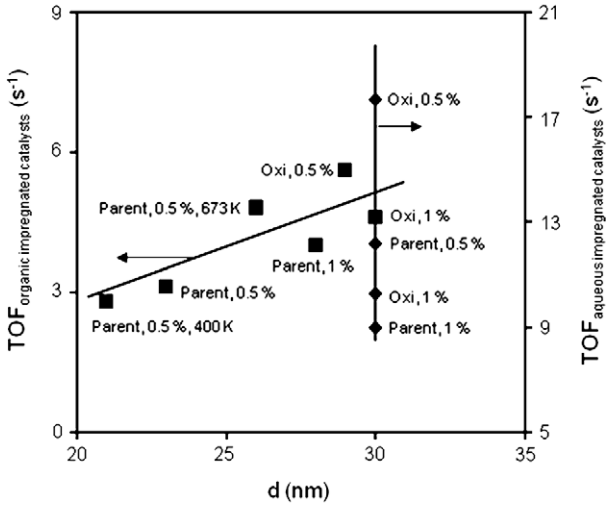

Fig. 8. TOF of fresh aqueous (♦) and organic (■) impregnated catalysts as function of the particle diameter.

In the case of the catalysts prepared from aqueous solution, it is observed that there are important variations on the catalyst activity although the metal dispersion does not vary significantly. These results indicate that there are more phenomena taking place at the catalytic surface and involving the support. Considering that the catalytic reaction needs the presence of palladium to occur (negligible conversions were obtained with both the parent and the activated nanofibres at 623 K), two different spill-over effects could take place. The first one is the spill-over of the TTCE from the carbonaceous material to the Pd particle; this effect will lead to higher local concentrations of TTCE on the surrounding of the Pd particles increasing the catalytic activity. At this point, previous works of our group showed that the adsorption capacity of the CNFs largely decreases after the oxidative treatment [11], whereas in Fig. 8, it is observed that for a given metal load and dispersion catalysts prepared from the oxidised precursor present better performance than those prepared from parent CNF. Therefore, it could be concluded that this effect is not relevant in our case. At this point, Amorim and Keane [48], studying the hydrodechlorination of chlorobenzenes over mechanical mixtures of Pd and CNFs and activated carbons with different concentration of functional groups found that the strong adsorption of the chlorinated compound on the acid functional groups of the carbon materials lead to reaction inhibition, discarding any kind of mobility of this adsorbed species.

The other spill-over effect that could take place is the diffusion of atomic hydrogen from the metal to the support, extending the surface at which the reaction would take place (although it is assumed that the reaction needs the presence of Pd for occurring, it takes place on the support in the vicinity of the Pd crystallites). It is assumed that the presence of inorganic hydrogen containing groups, such as the hydroxyl groups in the alumina-supported catalysts can promote this kind of spill-over effects, altering the

Table 3
Summary of the conversions obtained and resulting TOFs (estimated from Pd dispersion measured by XRD) for the fresh catalysts and the catalysts after 108,000 s on stream for the hydrodechlorination of TTCE at 523 K and 0.5 MPa.

Catalyst	$X_{initial}$ (%)	X_{final} (%)	$TOF_{initial}$ (s^{-1})	TOF_{final} (s^{-1})
0.5% Pd–CNF-aq	47	5	12.3	1.6
1% Pd–CNF-aq	69	5	9.2	1.2
0.5% Pd–CNF-oxi-aq	68	12	17.8	3.7
1% Pd–CNF-oxi-aq	79	5	10.4	0.7
0.5% Pd–CNF-org	16	3	3.1	1.2
1% Pd–CNF-org	33	18	4.2	3.5
0.5% Pd–CNF-oxi-org	23	10	5.6	3.2
1% Pd–CNF-oxi-org	46	21	4.6	3.5
0.5% Pd–CNF-org[a]	17	2	2.8	0.5
0.5% Pd–CNF-org[b]	23	9	4.8	3.4
1% Pd–CNF-org + CNF	33	17	4.0	3.4
1% Pd–CNF-org + CNF-oxi	40	23	4.9	4.6

[a] Catalyst reduced at 400 K.
[b] Catalyst reduced at 673 K.

reducibility of oxidised supports or modifying selectivities in hydrogenation reactions [49]. Thus, protonated functional groups of carbonaceous materials play a similar role in these materials. The impregnation of the materials with acid aqueous solution would promote the formation of these sites in a larger extent than the impregnation with an organic solvent. In a good agreement with this interpretation, catalysts prepared over the oxidised supports (higher concentration of functional groups) present higher initial TOF than the catalyst prepared from the parent CNFs. The evidences of these spill-over effects are even stronger if the hydrogen adsorption capacity is considered. So, whereas activated nanofibres show lower adsorption capacities than the parent materials, palladium addition has a marked influence on the adsorption properties of the oxidised materials. It is especially remarkable the effect of this addition when aqueous precursor is used (more than five times than the parent material), suggesting that these spill-over effects are enhanced by the preparation method selected. Experiments carried out with mechanical mixtures of the 1% Pd/CNF-org and CNF also suggest that the spill-over of hydrogen species in the surface active sites of the activated CNF is important, since the addition of activated CNF to the catalysts improves its performance, whereas the addition of the parent CNF has not any noticeable effect on catalyst performance.

The initial TOF is correlated with the Cl/Pd and the Pd^{2+}/Pd^0 ratios obtained by XPS, Fig. 9. It is observed that the initial activity of the catalysts (expressed as mole of TTCE converted per Pd atom and second) increases as the chlorine content of the catalyst increases for the samples prepared using the aqueous precursor, whereas this parameter has not any clear influence on initial TOF for the samples prepared using organic precursor. This fact suggests that the preparation method plays a more determinant role in the catalyst intrinsic activity than the CNF chemical activation.

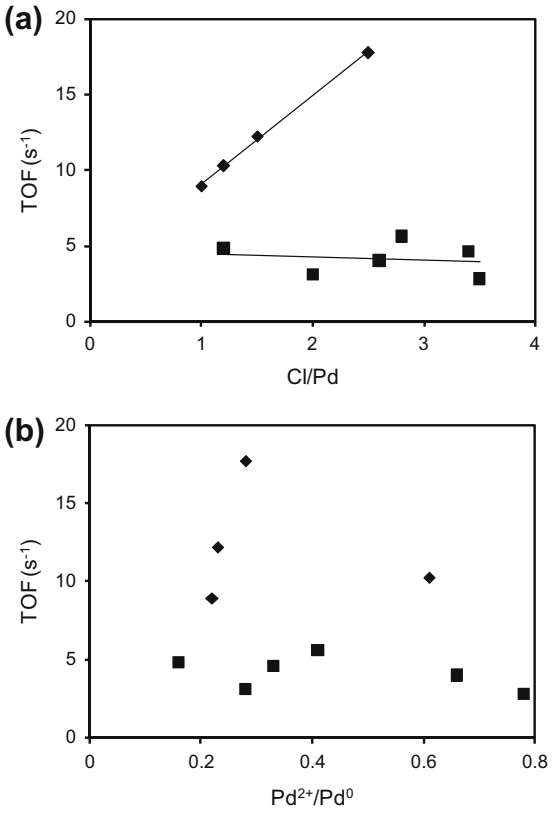

Fig. 9. TOF as function of Cl/Pd mole ratio (a) and Pd^{2+}/Pd^0 mole ratio (b) for: aqueous (♦) and organic (■) impregnation.

Regarding to the Pd^{2+}/Pd^0, two different trends are observed for the catalysts prepared from organic and aqueous precursor. In both cases, initial TOF increases as Pd^{2+}/Pd^0 increases reaching a maximum and decreases for the highest ratio. Similar behaviour has been found by Gomez-Sainero et al. [35] for liquid-phase hydrodechlorination of CCl_4 over palladium catalysts, although the maximum was obtained at higher Pd^{2+} concentrations (Pd^{2+}/Pd^0 ratio about 1.5), whereas in this work the maximum occurs at about 0.3 for the catalysts prepared from organic precursor and 0.5–0.6 for the catalysts prepared from aqueous precursor. This difference can also be explained considering the above-mentioned importance of the spill-over effects, so these authors used activated carbon supported catalysts, with higher concentration of functional groups that can contribute to the storage of hydrogen atoms, needing lower concentration of Pd^0 for this purpose.

Results obtained about the effect of chlorine and the palladium oxidation state can be explained from the point of view of the palladium coordination chemistry: although it is assumed that hydrogen is dissociatively chemisorbed on reduced palladium [50], the mechanism of the chlorinated hydrocarbon adsorption is not so clear. In the case of chloro-olefins, the most reasonable adsorption mechanism will involve the interaction of the C–C double bond with the Pd atom. This interaction is different in Pd^0 and Pd^{2+} atoms. In the first case, the olefin–metal interaction will be electron rich and susceptible to electrophilic attack (reaction with electropositive molecules or atoms), whereas in the second case, the olefin–metal complex is electron poor, especially when the olefin has very electronegative substituents, and consequently susceptible to nucleophilic attack by chemisorbed hydrogen atoms or hydrides. According to this mechanism, chlorine has several beneficial effects on the catalyst performance at this stage: it is a strong electron-acceptor atom, becoming the olefin–palladium complex even more electron poor, and it is a good outgoing group for the adsorption of TTCE on the Pd^{2+} sites. A reaction scheme formally similar to the mechanism proposed for the homogeneous Wacker reaction [51] can be proposed, the TTCE would form a complex with the Pd^{2+}, probably scavenging a chloride ion, and this complex will be attacked by the hydrogen, starting the hydrodechlorination reaction. Presumably, each Cl–H exchange is accomplished by the reduction of the Pd^{2+} to Pd^0 (as in the case of the Wacker reaction), but the Pd^0 can be re-oxidised by the protons released in the reaction. The increase in the Pd^{2+}/Pd^0 ratio during hydrodechlorination reactions has been found by other authors in the literature both in gas and aqueous phase [35]. The unexpected (if the redox potentials for the H^+/Pd pair are considered) high stability of electron-deficient palladium species in reductive environments when chloride and proton ions are present in the solid has already been reported in the literature [52]. It is assumed that this behaviour is caused by the interaction of Pd^0 with neighbouring protons (arising from the HCl generated during the reaction in this case). The presence of chloride ions stabilizes this system, hence promoting the oxidation. This effect has been proposed in the literature for both hydrodechlorination reactions and for explaining the abnormal reduction properties of catalysts prepared from chlorine-containing precursors [52].

The evolution of the TOF after 108,000 s on stream with the palladium crystallite size does not show any clear trend, although the TOF obtained for the aged catalysts is lower than the corresponding to the fresh catalysts in all the cases. Therefore, sintering effects are discarded as the only cause of catalysts deactivation, in spite of the increase in the average crystallite size observed in all the studied catalysts.

XPS characterisation results are especially important to determine the poisoning effects caused by the HCl released during the reaction. As previously discussed, the oxidation state of the Pd, as well as the local concentration of chlorine ions at the neighbouring

of the active phase, plays a key role in the activity of the catalyst. In order to elucidate these effects during the catalyst ageing, the ratio between the TOF of each aged and fresh catalyst is plotted versus the quotient between Pd^{2+}/Pd^0 ratio of the used and fresh catalyst (Fig. 10a), the concentration of inorganic chlorine (low binding energy chlorine) ratio (Fig. 10b) and the total amount of organic chlorine in the deactivated catalysts, since the concentration of this chlorine in the fresh catalysts is negligible (Fig. 10c). For comparison purposes, these properties were also normalised, when possible, taking the freshly reduced catalysts as reference.

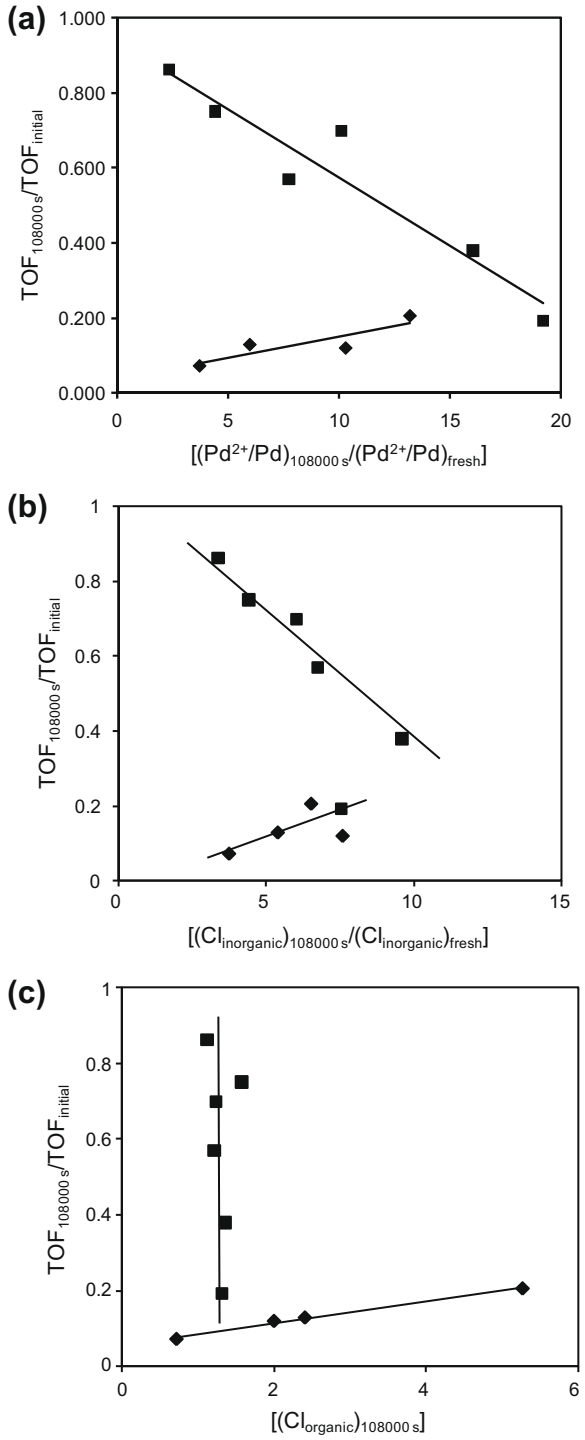

Fig. 10. Evolution of the ratio between the TOF after 108,000 s on stream and the initial TOF for aqueous (♦) and organic (■) impregnated catalysts with: (a) the ratio $[(Pd^{2+}/Pd^0)_{used}/(Pd^{2+}/Pd^0)_{fresh}]$; (b) the ratio $[(Cl_{inorganic})_{used}/(Cl_{inorganic})_{fresh}]$; and (c) the atomic concentration of organic chlorine after 108,000 s.

The evolution of the Pd^{2+}/Pd^0 ratio is completely different for the catalysts prepared from organic and from aqueous solutions. In the former case, the Pd^{2+}/Pd^0 ratios are always higher for the used catalysts, and there is a correlation between the increase in the concentration of Pd^{2+} and the activity loss (Fig. 10a). By contrast, this trend does not exist for the catalyst prepared from aqueous solutions. Similar behaviour has been observed for the evolution of the inorganic chlorine concentration (Fig. 10b); the increase in chlorine concentration being well correlated with activity losses for the catalysts prepared from organic precursors (with the exception of the Pd/CNF catalyst reduced at 400 K; probably because of its high initial chlorine concentration), whereas in the case of the catalysts prepared from aqueous supports, this chlorine has even a slightly positive effect. The observed trends for the catalysts prepared from organic precursors suggest that the activity losses in these catalysts is caused by HCl poisoning, which lead to increases in the surface concentrations of Pd^{2+} and Cl.

Regarding to the influence of the organic chlorine (Fig. 10c), there are two different possible sources of this organic chlorine: the presence of chlorine in the coke deposits (detected by TPO–MS for the catalysts prepared from aqueous solutions, as well as for coke deposits on conventional Pd catalysts used for this reaction [6,7,32]) and the presence of chlorine ions strongly adsorbed in the CNFs. At this point, Brichka et al. [53] observed the introduction of HCl molecules into the carbon nanotubes prepared from dichloromethane (in the defects of the graphene layers), stating that the presence of chlorine atoms in these materials markedly changed their adsorption properties.

Concerning the correlation between the concentration of this organic chlorine and the activity loss, no trend was observed for the catalysts prepared from organic precursor, whereas a slight positive effect of this chlorine on the residual activity was found for the catalysts prepared from aqueous solutions. This last point can be explained by different causes: the abovementioned spill-over effects (since this chlorine is in the support, favouring hydrogen adsorption or/and spill-over effects) or just because these catalysts are more active, transforming more molecules per time period, also for the coking reaction.

Taking into account all these facts, as well as the TPO–MS results, it is concluded that the main deactivation cause for the catalysts prepared from aqueous solutions is the formation of coke. Obtained results suggest that the preparation method plays a key role in the chemical properties of the catalysts, even more important than the chemical activation of the support. So, catalysts prepared from aqueous solutions present an enhanced surface chemistry, probably favouring hydrogen spill-over effects (leading to higher initial activities for similar values of the dispersion) and providing active sites for coke formation (leading to faster deactivation).

5. Conclusions

We have demonstrated in this work that both the surface treatment and, more markedly, the solvent used in the preparation of the palladium catalysts play a key role in the activity and deactivation behaviour of the catalysts. These differences are not mainly caused by the dispersion of the resulting catalyst, but by the surface chemistry of the support (presence/absence of functional groups, polarity, and protonation of these groups, etc.) and the active phase. In this case, the presence of chloride anion and the Pd^{2+}/Pd ratio determine the activity of the catalyst.

These parameters also determine the pre-eminence of the different deactivation causes, being observed different causes for

the deactivation of the catalysts prepared from aqueous solutions (fouling) and organic solutions (chlorine poisoning).

Acknowledgments

Marta León is acknowledged by her help in the experiments reported in this work. This work was supported by the Spanish Ministry for Science and Technology (Contract CTQ2005-09105-C04-04/PPQ). R.F. Bueres and E. Asedegbega-Nieto thank the Spanish Ministry of Education and Science for a Ph.D. Fellowship and "Juan de la Cierva" program, respectively.

References

[1] Toxicological Profile for Trichloroethylene and Tetrachloroethylene, Agency for Toxic Substances and Disease Registry (ATSDR), Department of Health and Human Services, Public Health Service, Atlanta, GA, 1997.
[2] European Commission, Reference Document on Best Available Techniques for Waste Treatment, Seville, 2005. <http://eippcb.jrc.es/pages/FActivities.htm>.
[3] S. Ordoñez, F.V. Díez, H. Sastre, Appl. Catal. B 25 (2000) 49.
[4] E. López, S. Ordóñez, F.V. Díez, Appl. Catal. B 62 (2006) 57.
[5] E. López, F.V. Díez, S. Ordóñez, Appl. Catal. B 82 (2008) 264.
[6] S. Ordóñez, F.V. Díez, H. Sastre, Appl. Catal. B 31 (2001) 113.
[7] S. Ordóñez, F.V. Díez, H. Sastre, Appl. Catal. B 40 (2003) 119.
[8] C. Amorim, G. Yuan, P.M. Patterson, M.A. Keane, J. Catal. 234 (2005) 268.
[9] R.F. Bueres, E. Asedegbega-Nieto, E. Díaz, S. Ordóñez, F.V. Díez, Catal. Commun. 9 (2008) 2080.
[10] M.L. Toebes, J.A. van Dillen, K.P. de Jong, J. Mol. Catal. A 173 (2001) 75.
[11] M.R. Cuervo, E. Asedegbega-Nieto, E. Díaz, A. Vega, S. Ordóñez, E. Castillejos-López, I. Rodríguez-Ramos, J. Chromatogr. A 1188 (2008) 264.
[12] M. Gurrath, T. Kuretzky, H.P. Boehm, L.B. Okhlopkova, A.S. Lisitsyn, V.A. Likholobov, Carbon 38 (2000) 1241.
[13] J.P. Brunelle, Pure Appl. Chem. 50 (1978) 1211.
[14] E. Díaz, S. Ordóñez, A. Vega, J. Colloid Interface Sci. 305 (2007) 7.
[15] S. Ordóñez, H. Sastre, F.V. Díez, J. Hazard. Mater. 81 (2001) 103.
[16] C.D. Wagner, W.M. Riggs, L.E. Davis, J.F. Moulder, G.E. Muilemberg, Handbook of X-ray Photoelectron Spectroscopy, Perkin Elmer Corp., Eden Prairie, MI, 1979.
[17] C.-H. Chen, C.-C. Huang, Micropor. Mesopor. Mater. 109 (2008) 549.
[18] C. Amorim, M.A. Keane, J. Colloid Interface Sci. 322 (2008) 196.
[19] F. Pinna, F. Menegazzo, M. Signoretto, P. Canton, G. Fagherazzi, N. Pernicone, Appl. Catal. A 219 (2001) 195.
[20] M. Makkee, E.J.A.X. van de Sandt, A. Wiersma, J.A. Moulijn, J. Mol. Catal. A 134 (1998) 191.
[21] S. Hermans, M. Kataoka, F. Nishiyama, H. Yasud, Carbon 38 (2000) 899.
[22] B.L. Mojet, M.S. Hoogenraad, A.J. van Dillen, J.W. Geus, D.C. Koningsberger, J. Chem. Soc., Faraday Trans. 93 (1997) 4371.
[23] P.A. Simorov, A.V. Romanenko, I.P. Prosvirin, E.M. Moroz, A.I. Boronin, A.L. Chuvilin, V.A. Likholobov, Carbon 35 (1997) 73.
[24] C. Prado-Bruguete, A. Linares-Solano, F. Rodríguez-Reinoso, C. Salinas-Martínez de Lecea, J. Catal. 115 (1989) 98.
[25] E. Díaz, S. Ordóñez, A. Vega, J. Coca, Micropor. Mesopor. Mater. 82 (2005) 173.
[26] J. González, M.delC. Ruiz, A. Bohé, D. Pasquevich, Carbon 37 (1999) 1979.
[27] L. Calvo, M.A. Gilarranz, J.A. Casas, A.F. Mohedano, J.J. Rodríguez, Appl. Catal. B 67 (2006) 68.
[28] K. Foger, D. Hay, H. Jaeger, J. Catal. 96 (1985) 154.
[29] S.B. Ziemecki, G.A. Jones, J. Catal. 95 (1985) 621.
[30] S.B. Ziemecki, D.G. Schwarzfager, G.A. Jones, J. Am. Chem. Soc. 107 (1985) 4547.
[31] E.J. Creyghton, M.H.W. Burgers, J.C. Janssen, H. van Bekkum, Appl. Catal. A 128 (1995) 275.
[32] S. Ordóñez, H. Sastre, F.V. Díez, Thermochim. Acta 379 (2001) 25.
[33] G. Kumar, J.R. Blackburn, M.M. Jones, R.G. Albridge, W.E. Moddeman, Inorg. Chem. 11 (1972) 296.
[34] R. Gopinath, N. Lingaiah, B. Sreedhar, I. Suryanarayana, P.S. Sai Prasad, A. Obuchi, Appl. Catal. B 46 (2003) 587.
[35] L. Gomez-Sainero, X.L. Seoane, J.L.G. Fierro, A. Arcoya, J. Catal. 209 (2002) 279.
[36] X.L. Seoane, P.C. L'Argentiere, N.S. Fígoli, A. Arcoya, Catal. Lett. 16 (1992) 137.
[37] L.E. Pimentel Real, A.M. Ferraria, A.M. Botelho do Rego, Polym. Test. 26 (2007) 77.
[38] J.J.F. Scholten, A.P. Pijpers, A.M. L Hustings, Catal. Rev. Sci. Eng. 27 (1985) 151.
[39] S. Lambert, J.F. Polard, J.P. Pirard, B. Heinrichs, Appl. Catal. B 50 (2004) 127.
[40] C.A.G. Sánchez, C.O.M. Patiño, C.M. de Correa, Catal. Today 133–135 (2008) 520.
[41] M.O. Nutt, K.N. Heck, P. Álvarez, M.S. Wong, Appl. Catal. B 69 (2006) 115.
[42] W. Juszczyk, A. Malinowski, Z. Karpinski, Appl. Catal. A 166 (1998) 311.
[43] F.H. Ribeiro, C.A. Gerken, G. Rupprechter, G.A. Somorjai, C.S. Kellner, G.W. Coulston, L.E. Manzer, L. Abrams, J. Catal. 176 (1998) 352.
[44] G.C. Bond, Chem. Soc. Rev. 20 (1991) 441.
[45] M. Boudart, G. Djega-Mariadassou, Kinetics of Heterogeneous Catalytic Reactions, Princeton University Press, 1984 (pp. 155–191).
[46] J.A. Dumesic, H. Topsøe, S. Khammouma, M. Boudart, J. Catal. 37 (1975) 513.
[47] D.J. Moon, M.J. Chung, K.Y. Park, S.I. Hong, Appl. Catal. A 168 (1998) 159.
[48] C. Amorim, M.A. Keane, J. Chem. Technol. Biotechnol. 83 (2008) 662.
[49] Z. Yu, L.E. Fareid, K. Moljord, E.A. Blekkan, J.C. Walmsley, D. Chen, Appl. Catal. B 84 (2008) 482.
[50] J.M. Driessen, E.K. Poels, J.P. Hindermann, V. Ponec, J. Catal. 82 (1983) 26.
[51] R.F. Heck, Palladium Reagents in Organic Synthesis, Academic Press, London, 1985.
[52] Z. Karpinski, Adv. Catal. 37 (1990) 45.
[53] S.Y. Brichka, G.P. Prikhod'ko, Y.I. Sementsov, A.V. Brichka, G.I. Dovbeshko, O.P. Paschuk, Carbon 42 (2004) 2581.